Bam35 Tectivirus Intraviral Interaction Map Unveils New Function and Localization of Phage ORFan Proteins

Mónica Berjón-Otero,[a] Ana Lechuga,[a] Jitender Mehla,[b] Peter Uetz,[b] Margarita Salas,[a] Modesto Redrejo-Rodríguez[a]

Centro de Biología Molecular Severo Ochoa, Consejo Superior de Investigaciones Científicas y Universidad Autónoma de Madrid, Madrid, Spain[a]; Center for the Study of Biological Complexity, Virginia Commonwealth University, Richmond, Virginia, USA[b]

ABSTRACT The family *Tectiviridae* comprises a group of tailless, icosahedral, membrane-containing bacteriophages that can be divided into two groups by their hosts, either Gram-negative or Gram-positive bacteria. While the first group is composed of PRD1 and nearly identical well-characterized lytic viruses, the second one includes more variable temperate phages, like GIL16 or Bam35, whose hosts are *Bacillus cereus* and related Gram-positive bacteria. In the genome of Bam35, nearly half of the 32 annotated open reading frames (ORFs) have no homologs in databases (ORFans), being putative proteins of unknown function, which hinders the understanding of their biology. With the aim of increasing knowledge about the viral proteome, we carried out a comprehensive yeast two-hybrid analysis of all the putative proteins encoded by the Bam35 genome. The resulting protein interactome comprised 76 unique interactions among 24 proteins, of which 12 have an unknown function. These results suggest that the P17 protein is the minor capsid protein of Bam35 and P24 is the penton protein, with the latter finding also being supported by iterative threading protein modeling. Moreover, the inner membrane transglycosylase protein P26 could have an additional structural role. We also detected interactions involving nonstructural proteins, such as the DNA-binding protein P1 and the genome terminal protein (P4), which was confirmed by coimmunoprecipitation of recombinant proteins. Altogether, our results provide a functional view of the Bam35 viral proteome, with a focus on the composition and organization of the viral particle.

IMPORTANCE Tailless viruses of the family *Tectiviridae* can infect commensal and pathogenic Gram-positive and Gram-negative bacteria. Moreover, they have been proposed to be at the evolutionary origin of several groups of large eukaryotic DNA viruses and self-replicating plasmids. However, due to their ancient origin and complex diversity, many tectiviral proteins are ORFans of unknown function. Comprehensive protein-protein interaction (PPI) analysis of viral proteins can eventually disclose biological mechanisms and thus provide new insights into protein function unattainable by studying proteins one by one. Here we comprehensively describe intraviral PPIs among tectivirus Bam35 proteins determined using multivector yeast two-hybrid screening, and these PPIs were further supported by the results of coimmunoprecipitation assays and protein structural models. This approach allowed us to propose new functions for known proteins and hypothesize about the biological role of the localization of some viral ORFan proteins within the viral particle that will be helpful for understanding the biology of tectiviruses infecting Gram-positive bacteria.

KEYWORDS tectivirus, Bam35, yeast two-hybrid, intraviral interactome, ORFan, protein-protein interactions, PPIs

Viruses within the *Tectiviridae* family can be divided into lytic bacteriophages preying on diverse gammaproteobacteria (e.g., PRD1) (1) and temperate phages whose hosts are Gram-positive bacteria belonging to the *Bacillus cereus sensu lato* group (reviewed in reference 2). The latter comprises bacteriophages that infect *B. thuringiensis*, such as Bam35, Gil01, and Gil16 (3); *B. anthracis*, such as AP50 and Wip1 (4, 5); and *B. cereus*, such as Sole or Simila (6, 7). Contrary to most temperate bacteriophages, members of this group are not integrative viruses; rather, they replicate as linear episomic plasmids during the lysogenic cycle (8), in which late phage functions are suppressed (9). Further, they are also closely related to the *B. cereus* linear plasmid pBClin15 (8). Interest in the study of tectiviruses of Gram-positive bacteria has increased in the last few years due to the narrow host specificity of some of them for dangerous human pathogens (10, 11), their complex diversity and variability patterns (2, 7), and their possible phylogenetic relationship with some groups of eukaryotic viruses and mobile elements (12, 13). However, they remain less well-known than the PRD1-related bacteriophages.

Tectiviruses have a tailless icosahedral structure with flexible spikes extending from their vertices. The capsid encloses an inner membrane, which is an unusual feature in bacterial viruses. This membrane is formed of approximately equal amounts of virus-encoded proteins and lipids derived from the host cell plasma membrane (14). Cryo-electron microscopy and image reconstruction of bacteriophage Bam35 revealed that this phage and PRD1 are structurally very similar, with their major structural difference being the thickness and curvature of their membranes, probably due to the differences in the integral membrane proteins (15–18). Thus, the coat proteins of Bam35, like those of PRD1, are organized on a pseudo T=25 lattice, with 240 trimers of the major capsid protein forming the facets of the viral particle. In both phages, the size of the capsid is determined by dimers of a tape measure protein (also referred as the minor capsid protein) running between adjacent facets connecting the vertices (17, 19). Eleven of the 12 vertices showed a protein complex, the viral penton, in which the spikes are anchored. The spike proteins are required for host recognition and are stabilized by a small protein that links the spike complex to the membrane in the PRD1 viral particle. The cryo-electron microscopy image of the Bam35 viral particle reveals a density cloud analogous to that protein (17, 20). The 12th vertex of the viral capsid is called the unique vertex and contains the viral machinery required for DNA packaging and injection (21). The viral particles of PRD1 and Bam35 are also associated with proteins having peptidoglycan-hydrolyzing activity (22–26).

Finally, the lipid membrane encloses an approximately 15-kb linear double-stranded DNA genome with inverted terminal repeat sequences that is replicated by a protein-primed mechanism (27–29). This mechanism is specific to linear genomes and has been well characterized in the podovirus Φ29 (30, 31) but also in linear plasmids and other virus groups, including tectiviruses and adenoviruses (27, 29, 32, 33). Protein-primed replication starts by the formation of a phosphoester bond, catalyzed by the viral DNA polymerase (DNAP), between the first nucleotide and the OH group of a serine, threonine, or tyrosine residue of a protein (the terminal protein [TP]) that acts as a primer and becomes covalently bound to both 5′ ends of DNA (TP-DNA). Despite belonging to the same family, PRD1 and Bam35 show differences in this step of replication. Thus, the PRD1 initiation step involves the reiterative copy of the fourth base of a 3′-CCCC terminal repeat, and it requires that the initiation products [TP-(dGMP)$_n$] translocate backwards in three consecutive sliding-back steps to recover DNA end information (28). On the contrary, Bam35 initiation is directed by the third base of the 3′-ATA genome end, and a subsequent third-to-first template base single-nucleotide jumping-back process may be responsible for the recovery of the information of the 3′ end sequence (29). Then, in both cases, the DNAP resumes the genome replication coupling strand displacement and processive DNA synthesis (29, 34, 35). Full-length TP-DNA replication can be achieved *in vitro* only with two proteins, namely, TP and DNAP (29, 34, 36). However, the presence of additional factors, like single- and double-stranded DNA-binding proteins, strongly stimulates the replication of PRD1 (37,
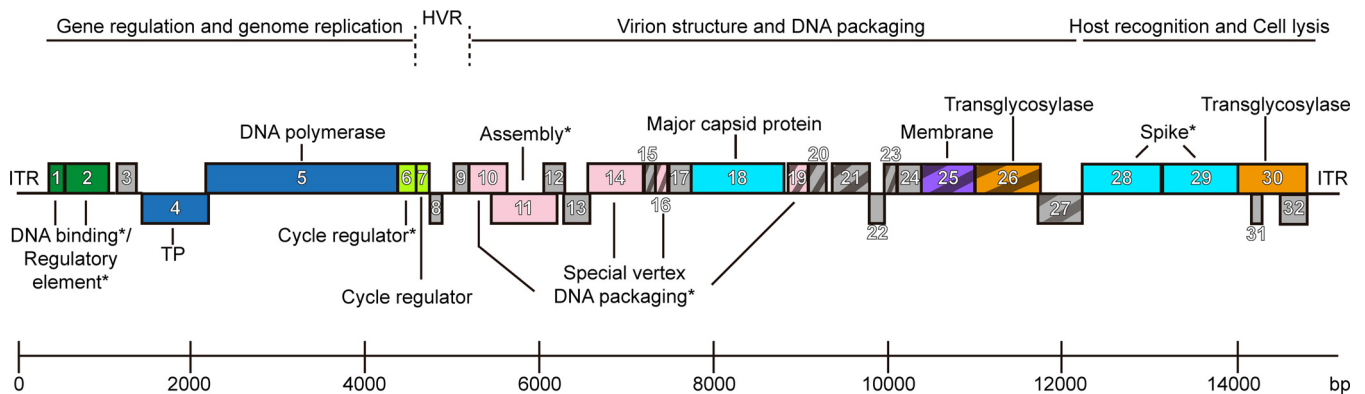
FIG 1 Genetic map of phage Bam35. The boxes correspond to the ORFs predicted to exist in the Bam35 genome. The ORFs that overlap another ORF(s) are represented at the bottom. Namely, the last 5 amino acids of ORF4 overlap ORF5, the last 8 amino acids of ORF7 overlap ORF8, the last 62 amino acids of ORF10 and the first 51 amino acids of ORF12 overlap ORF11, the last 10 amino acids of ORF12 and the first 6 amino acids of ORF14 overlap ORF13, the last amino acid of ORF21 and first amino acid of ORF24 overlap ORF23, the last 17 amino acids of ORF26 overlap ORF27, ORF31 is constituted by nucleotides 148 to 527 (in +1 frame) of ORF30, and ORF32 is constituted by the 102 C-terminal amino acids of ORF30. The previously shown or suggested (*) function of the protein or the type of protein encoded by an ORF is indicated as follows: green, DNA-binding protein; blue, DNA replication; chartreuse, cycle regulator; salmon, assembly or DNA packaging and other special vertex components; cyan, major capsid and spike proteins; purple, membrane structural protein; and orange, lytic proteins. Oblique lines indicate a predicted transmembrane domain. The ruler at the bottom represents the number of base pairs in the Bam35 genome. ITR, inverted terminal repeat; HVR, highly variable region. See Table S1 in the supplemental material for further details.

38). Orthologs of these proteins in Bam35 have not yet been experimentally characterized.

Although their genome organizations are similar, tectiviruses infecting Gram-negative and Gram-positive bacteria share almost no sequence identity at the nucleotide level (39, 40). Therefore, the proteins encoded by most of the annotated open reading frames (ORFs) of Bam35 show no similarities with known proteins in databases and are known as ORFan proteins. Only a few of these proteins of unknown function have proposed biological roles that were suggested on the basis of low levels of protein similarity and synteny (39). Furthermore, multiple-sequence alignments and the hidden Markov model profiles of proteins recently published in databases did not reveal any new functions for Bam35 proteins (41, 42). As a consequence and despite the availability of the structures of the Bam35 particles, 15 out of 32 predicted proteins encoded by the Bam35 genome are ORFans of unknown function (Fig. 1; see also Table S1 in the supplemental material).

Intraviral interactomes have been generated by screening of the protein-protein interactions (PPIs) of viral proteins and can help provide an understanding of their role in biological processes. Interactomes provide new insights into protein function unattainable by studying proteins individually (43). Recently, different modifications of yeast two-hybrid (Y2H) screening have been made to reduce the rate of occurrence of false-positive and false-negative results (44). Briefly, a transcription factor, typically, the *Saccharomyces cerevisiae* yeast transcription factor Gal4, is split into a DNA-binding domain (DBD) and an activation domain (AD), which are independently fused to the protein of interest, producing the bait and prey proteins, respectively. PPIs are detected through the activation of a reporter gene as a consequence of the reconstitution of the transcription factor. One of the most commonly used reporters is the *HIS3* gene, which encodes the histidine biosynthetic enzyme imidazole glycerol phosphate (IGP) dehydratase, allowing the growth of histidine-auxotrophic yeast in the absence of this amino acid. This reporter allows the background due to the autoactivation of the proteins under study to be reduced through the addition of 3-amino-1,2,4-triazole (3AT), a competitive inhibitor of the His3 protein (see Materials and Methods) (43). This approach has been applied successfully to the study of phage interactomes from different hosts, including *Escherichia coli* bacteriophage λ, *Streptococcus* phage Cp-1, or *Mycobacterium* phage Giles (45–47).

We used this technique and present here a comprehensive intraviral interactome of

the tectivirus Bam35 to gain a further understanding of the viral replication cycle and structure. We identified a total of 76 unique interactions produced by 12 proteins with an established or predicted function and 12 ORFan proteins of unknown function. We further confirmed by coimmunoprecipitation one of the interactions between non-structural proteins (P1-TP), which was detected by the Y2H assay with only one combination of vectors. Analysis of the interactions map revealed new insights into proteins of known function, such as the conserved transglycosylase P26 (25, 26), which appeared to be a cornerstone membrane protein that interacts with other lytic proteins as well as with capsid and special vertex components. Moreover, we suggest possible functions and localizations for some viral ORFan proteins, including P15 and P22 as components of the special vertex, P17 as the capsid tape measure protein, and P24 as the penton component. The function of the last protein is supported by a structural model based on a PRD1 orthologue.

RESULTS

Bam35 ORF library construction and quality control. All predicted Bam35 ORFs (Fig. 1; see also Table S1 in the supplemental material) were cloned into the donor vector pDONR/Zeo and subsequently subcloned in two bait vectors, pGBKCg and pGBGT7g, and two prey vectors, pGADCg and pGADT7g, producing N- and C-terminal fusion proteins (see Materials and Methods for details) (44). Therefore, we tested the protein interactions in all possible conformations, reducing the number of false-negative results produced by structural constraints in fusion proteins (44, 45).

In addition, to avoid problems associated with membrane localization, proteins with potential transmembrane domains (boxes with oblique lines in Fig. 1) were identified using TMHMM software (48), and a short version of each of these proteins without those domains (identified by use of a prime symbol) was generated. Thereby, in addition to the 32 full-length ORFs, we cloned the short versions of ORFs 19, 20, 21, 25, 26, and 27, referred to as ORFs 19′, 20′, 21′, 25′, 26′, and 27′, respectively.

All constructs were successfully obtained, except ORF16 in pGBKCg and ORFs 9 and 26 in pGADCg (Table S4). The sequencing of the cloned ORFs in the donor vector showed that 5 of the proteins encoded by the Bam35 genome had a change of a single amino acid (Table S1). These mutations were detected in 3 out of 3 different clones analyzed, which may indicate either that mutations occurred at any step of amplification from the original isolate, that a sequencing error occurred in the original genome, or that mutations were introduced during the PCR and cloning procedures. The last possibility is favored by the fact that 4 out of 5 ORFs containing mutations (namely, those coding for P8, P10, P14, and P18) were identical in three independent isolates, Bam35, Gil01, and the recently sequenced plasmid pGil02 (49).

Protein-protein interactions were detected using *HIS3* as a reporter gene and 3-amino-1,2,4-triazole (3AT) as a competitive inhibitor (50) to reduce bait and prey autoactivation (Table S5; for details, see Materials and Methods). One prey protein, P24, was found to be an autoactivator in the vector pGADCg (Fig. 2A). As a consequence, the yeast clone transformed with pGADCg::ORF24 was excluded from our screens. Similarly, the prey protein P25 without a transmembrane domain (P25′) carried by pGADT7g interacted with 13 bait proteins carried by the pGBGT7g vector, although it did not show self-activation with the same empty bait vector (Fig. 2B). However, the P25′ prey protein was self-activating in combination with the empty bait vector pGBKCg (Fig. 2B). Therefore, since the protein P25′ is a short version of P25, which shows high levels of promiscuity and self-activation, we considered these interactions to be false positive.

The interactome of Bam35 determined by yeast two-hybrid screening. We detected 129 interactions in the initial screening. Each interaction was verified by a new analysis at different 3AT concentrations (0, 0.025, 0.1, 3, 10, 25, and 50 mM) at the same time that the self-activation of the prey and bait proteins was retested. The interactions were considered positive when the growth of the yeast expressing the combination of a prey protein with a bait protein of Bam35 was higher than that of the yeast that expressed only the prey protein or only the bait protein (negative controls) or when the
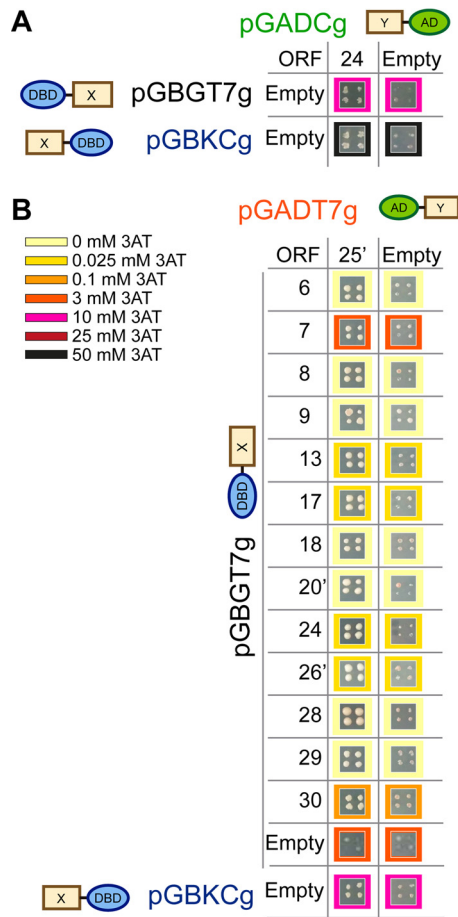
FIG 2 Criteria for observation of false-positive interactions in the yeast two-hybrid screening. (A) Representative images of the growth of the yeast transformed with the empty vector pGBGT7g or pGBKCg and the construct pGADCg::ORF24 at 10 and 50 mM 3AT, respectively. At the right, the growth of the yeast transformed with the empty vector pGBGT7g or pGBKCg and the empty vector pGADCg at the same 3AT concentrations is shown as a control. (B) Representative image of the interactions found between prey protein P25′ expressed from pGADT7g and the bait proteins of Bam35 expressed from pGBGT7g or the empty vector pGBKCg. At the right, the growth of the yeast that expresses the same bait protein from the vector pGBGT7g or the empty vector pGBKCg and the empty vector pGADT7g at the same 3AT concentrations is shown as a control. The schematic representation of each fusion protein expressed from the indicated vectors is indicated. X and Y, the bait and prey proteins encoded by the indicated Bam35 ORF, respectively (in the case of the empty vector, X and Y are absent). The 3AT concentrations are represented by the colored frame, and the colors are defined in the key.

growth of both was the same but the growth of the negative control gave rise to reddish colonies, indicative of impaired or stressed growth. Following these criteria, we confirmed a total of 112 interactions (Tables 1 and S6; Fig. 3), produced by 24 out of 32 Bam35 proteins (75% coverage). However, when redundant PPIs detected with different vector combinations were merged (Fig. 4), the final number of unique interactions could be reduced to 76. Remarkably, only 6 of these interactions may be expected or hypothesized on the basis of known protein functions (Table 1). The highest number of positive results was obtained with the proteins expressed from the combination of the vectors pGBGT7g and pGADT7g (fused at their N termini [NN]), followed by pGBGT7g and pGADCg (fused at the N terminus and C terminus, respectively [NC]), pGBKCg and pGADT7g (fused at their C terminus and N terminus, respectively [CN]), and pGBKCg and pGADCg (fused at their C termini [CC]) (Table S6; Fig. 3 and 4), which is in line with the results previously obtained for other bacteriophages (45, 46).

The intraviral interaction map is depicted in Fig. 5, where the nodes represent the 25 proteins that showed some interaction as well as indicate the established or

TABLE 1 Summary of PPIs obtained in the yeast two-hybrid screening[a]

Bait protein[b]	Prey protein	No. of vectors	Notes [reference(s)][c]
1 (DNA binding)	4	1	
3	3	2	
	17	1	
4 (TP)	4	2	A TP self-interaction was also reported for unrelated virus Φ29 and would be involved in the recruitment of a TP-DNAP heterodimer to the genome ends (31)
6 (cycle regulator)	3	1	
	6	1	
	8	1	
	9	1	
	24	2	
	29	2	
	30	1	
	32	1	
7 (cycle regulator)	7	4	
8	8	4	
9	9	2	
13	3	1	
	6	1	
	8	1	
	9	1	
	24	1	
	29	2	
	30	1	
	32	1	
14 (DNA packaging/ATPase)	14	2	Multimerization expected (17)
15	22	1	
17	17	4	
	18	2	
	24	1	
	29	2	
	30	1	
	32	1	
18 (major capsid protein)	18	1	Self-interaction was shown previously (17)
19 (DNA packaging)	22	1	
20′	3	1	
	24	1	
	29	1	
21	12	1	
22	22	1	
24	3	1	
	6	1	
	7	1	
	8	1	
	9	1	
	14	1	
	24	1	

TABLE 1 (Continued)

Bait protein[b]	Prey protein	No. of vectors	Notes [reference(s)][c]
	29	2	
	30	1	
	32	2	
25 (membrane structure)	17	1	
	24	1	
	29	1	
26 (transglycosylase)	21	2	
	22	1	
	26′	1	
26′	3	1	
	6	1	
	7	1	
	8	1	
	14	1	
	17	4	
	24	2	
	26′	1	
	29	2	
	30	2	
	32	2	
28 (spike)	17	2	
	28	3	Multimerization expected (17, 39)
29 (spike)	24	1	
	28	2	Expected interaction (17)
	29	2	
30 (transglycosylase)	6	1	
	24	1	
	29	2	
	30	2	
	32	2	
32	32	1	

[a]See Table S6 in the supplemental material for more detailed information.
[b]Previously shown or hypothesized functions for Bam35 proteins are indicated (see Table 2 for more detailed information).
[c]PPIs that have been shown previously or could be hypothesized on the basis of protein function are indicated.

postulated function of each protein. The type of line connecting the nodes indicates the number of vector combinations in which the interaction was observed, and their colors show the highest 3AT concentration tolerated by this interaction. The map obtained contains 12 ORFan proteins of unknown function, and the majority of the proteins with a proposed function are structural components of the Bam35 viral particle. In addition, some interactions involved proteins with a role in genome delivery or replication as well as in regulation of the viral cycle.

Direct interaction between recombinant viral TP and P1 proteins. As mentioned above, the Y2H screening also detected the interaction between TP and nonstructural protein P1 when they were expressed from pGADCg and pGBKCg, respectively (Table S6; Fig. 3D and 5).

Since this interaction was observed with only one vector combination, we decided to confirm it by a pulldown coimmunoprecipitation assay. Thus, both Coomassie staining and Western blotting (Fig. 6) showed that purified TP is retained when P1 tagged with hemagglutinin (HA) either at its N terminus (HA-P1) or at its C terminus (P1-HA) was bound to the column (Fig. 6A and B, lanes 14 and 21). However, the terminal protein flowed through the column when P1 was absent (Fig. 6A and B, lane
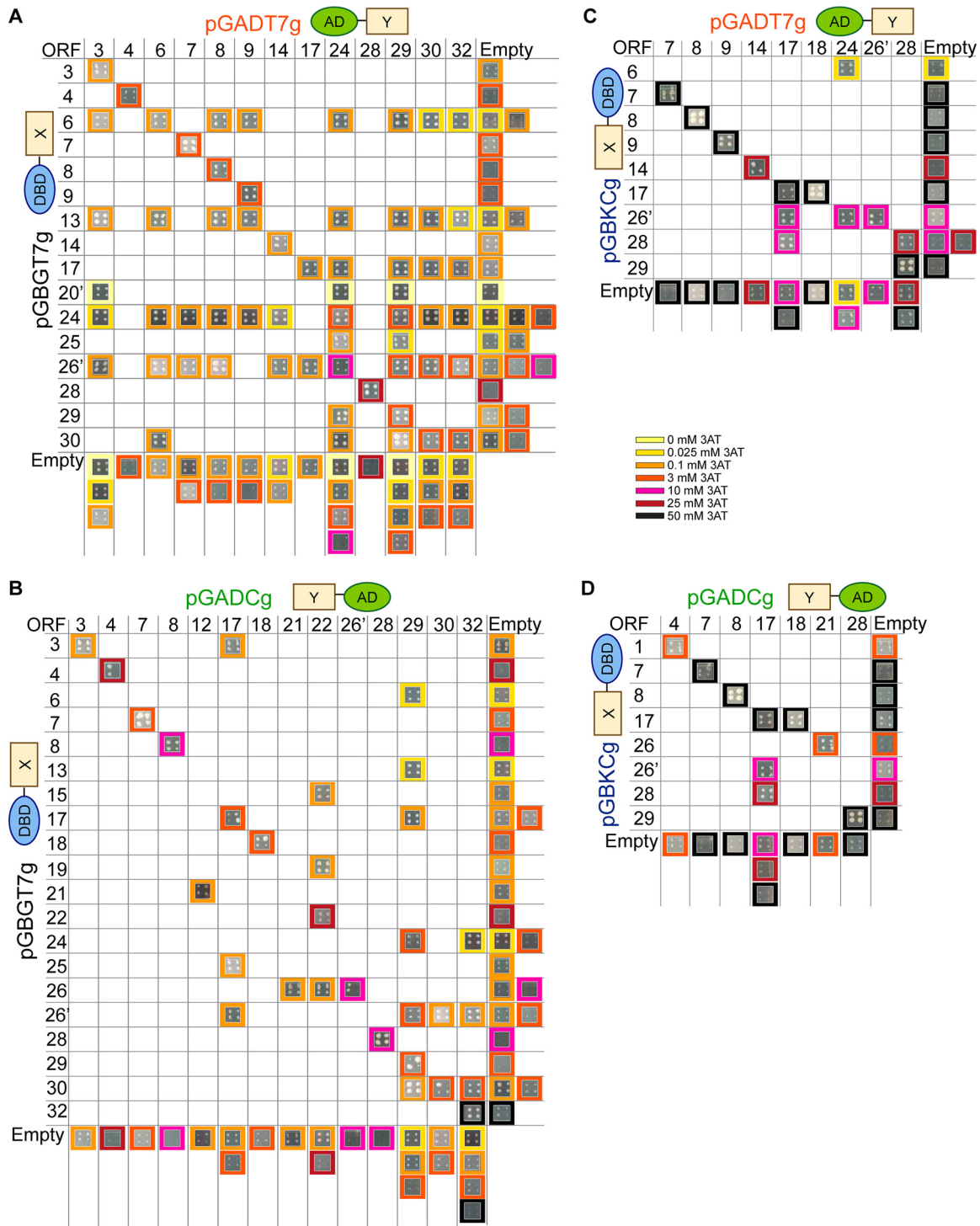
FIG 3 Matrix representation of the interactions between the Bam35 proteins detected. Positive results obtained with the vector combinations used, as well as the self-activation controls of the prey and bait proteins, are shown. (A) Positive interactions between the Bam35 proteins fused by their N-terminal ends to the domains of the Gal4 transcription factor (NN; pGBGT7g and pGADT7g vectors). (B) Positive interactions between the bait Bam35 proteins fused by their N-terminal ends to the DBD domain of the Gal4 transcription factor and the prey Bam35 proteins fused by their C-terminal ends to the AD domain (NC; pGBGT7g and pGADCg vectors). (C) Positive interactions between the bait Bam35 proteins fused by their C-terminal ends to the DBD domain of the Gal4 transcription factor and the prey Bam35 proteins fused by their N-terminal ends to the AD domain (CN; pGBKCg and pGADT7g vectors). (D) Positive interactions between the Bam35 proteins fused by their C-terminal ends to the domains of the Gal4 transcription factor (CC; pGBKCg and pGADCg vectors). The images in all the panels correspond to those obtained with the highest 3AT concentration at which the interaction was detected, as indicated by the colored frame. The controls for the self-activation of the bait proteins (yeast transformed with the combination pGBGT7g::ORF or pGBKCg::ORF and empty pGADT7g or empty pGADCg) as well as the self-activation of the prey proteins (empty pGBGT7g or empty pGBKCg with pGADT7g::ORF or pGADCg::ORF) at the same 3AT concentration are shown at the right and at the bottom.
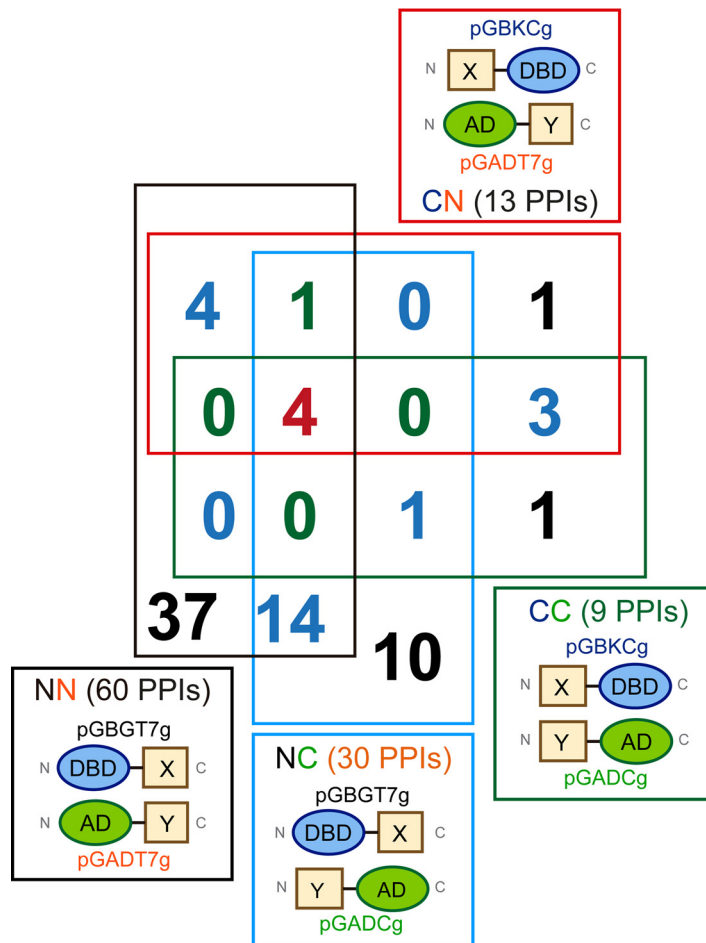
FIG 4 Bam35 interactions found by different combinations of bait/prey fusion proteins. The numbers of reproducible protein-protein interactions (PPIs) detected with four, three, two, and one different combinations of vectors are indicated in red, green, blue, and black, respectively. The combination of vectors used, a graphic representation of the fusion protein obtained in each case, and the number of PPIs detected with each combination are indicated inside the boxes. AD, activation domain of the Gal4 transcription factor; DBD, DNA-binding domain of Gal4 transcription factor.

5). These results confirm the direct interaction between P1 and TP and support the usefulness of the Y2H assay approach for the screening of intraviral PPIs to detect the interactions between nonstructural viral proteins.

DISCUSSION

Interactions of capsid and spike proteins. We detected several known or expected interactions, like the self-interaction of the major capsid protein P18 or the interaction between the suggested spike proteins P28 and P29 (17, 39), that validate the use of the yeast two-hybrid system to detect interactions between structural proteins of viruses (Table 1). The integration of the interactome obtained with the available information allows us to propose new protein functions (Table 2), as well as an updated model of the Bam35 virion structure (Fig. 7A).

Sozhamannan et al. (51) suggested that protein P24 of Bam35 and its homologs in related viruses were the capsid tape measure protein. However, the screening carried out in this study does not support that hypothesis because the tape measure and the major capsid proteins should interact in each capsid facet (17), but this interaction was not detected (Fig. 5). Conversely, our results showed that the P18 protein interacts with P17, which also showed self-interaction. This suggests that dimers of P17 could serve as the tape measure protein of the Bam35 bacteriophage capsid, similarly to PRD1 P30 dimers (19).
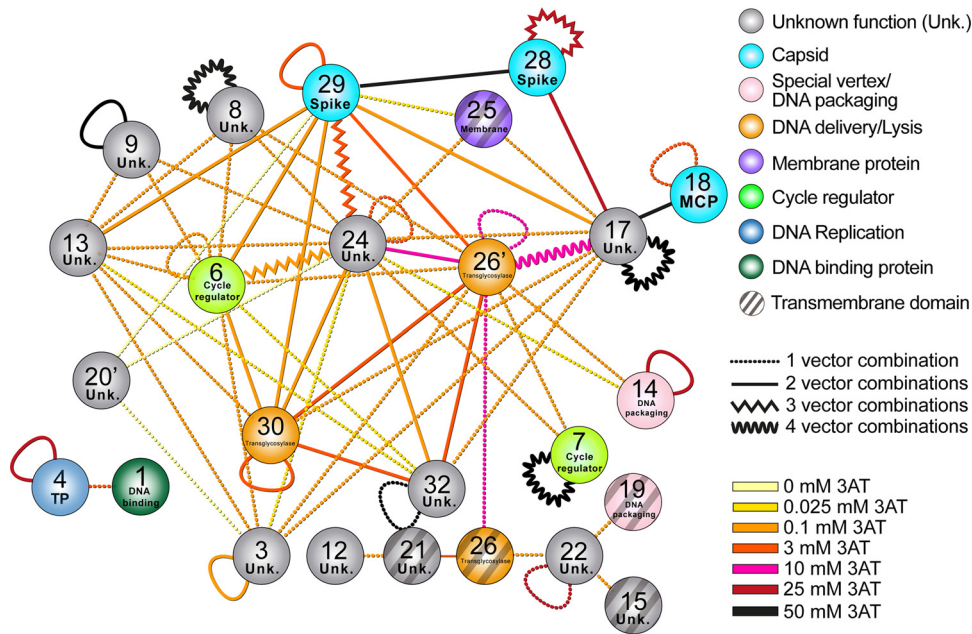
FIG 5 The protein interaction network of bacteriophage Bam35. The nodes represent the proteins that showed interactions, and the colors indicate the postulated or established functions, as defined in the legend to Fig. 1 (see the key at the right). The oblique lines indicate that a transmembrane domain has been predicted in these proteins. The nodes P20′ and P26′ correspond to the versions without transmembrane domains of P20 and P26, respectively. The lines connecting the nodes indicate the protein interactions. The pattern of the connector lines indicates the number of vector combinations in which the interaction was detected. Line colors indicate the highest 3AT concentration tolerated by each interaction.

Regarding the vertex penton, although it was suggested to be made up of protein P13 oligomers (17), the PPIs detected do not support that assumption due to the absence of an interaction of P13 with itself, which is required to generate pentamers (Fig. 5). On the other hand, taking into account the facts that the molecular mass of P24
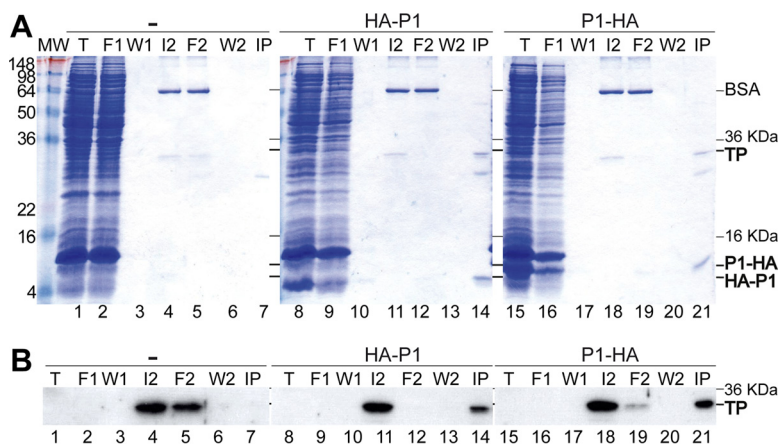

FIG 6 Direct interaction between recombinant proteins P1 and TP. HA-P1 and P1-HA were immunoprecipitated from *Escherichia coli* cell extracts expressing these proteins. Bacterial cells harboring the empty vector (−) were used as a negative control. Bound proteins were subsequently incubated with a mixture of purified TP (P4) and BSA to detect the direct P1-TP interaction. Equivalent volumes from each step were analyzed by 15% SDS-PAGE and visualized by Coomassie staining (A) or Western blotting (B) with antiserum against viral TP. Lane MW, molecular weight markers (the molecular weights [in thousands] are indicated to the left of panel A); lanes 1 to 7, results obtained using a cell extract of *E. coli* transformed with the empty pT7-7 vector; lanes 8 to 14, results obtained by coimmunoprecipitation using a cell extract of *E. coli* expressing the fusion protein HA-P1; lanes 15 to 21, results obtained with fusion protein P1-HA. T, total lysate input; F1 and W1, flowthrough and wash (third step) from the P1 immunoprecipitation with HA resin, respectively; I2, F2, W2, and IP, TP-BSA input, flowthrough, wash, and coimmunoprecipitated fraction from the TP pulldown, respectively. See Materials and Methods for details.

TABLE 2 Updated description of the annotated Bam35 ORFs[a]

ORF	Function	Length (no. of amino acids)	Reference(s) or source	Comments[c] (reference)
1	DNA binding[b]/regulatory protein[b]	58	58; this work	Gil01 phage with mutations in ORF1; interaction with TP suggests a role in genome replication
2	DNA binding/regulatory protein[b]	167	67	pBClin15 ortholog from preliminary characterization in cell extracts
3	Unknown	74		
4	TP	245	29	Recombinant protein characterization
5	DNA polymerase	735	35, 39	Sequence similarity and recombinant protein characterization
6	Cycle regulator[b]	66	39	Sequence similarity
7	Cycle regulator	50	59	Recombinant protein of identical Gil01 protein
8	Unknown	46		
9	Unknown	57		
10	DNA packaging[b]	145	39	PRD1 synteny and weak similarity
11	Assembly protein[b]	252	39	PRD1 synteny and weak similarity
12	Unknown	80		
13	Unknown	102		
14	DNA packaging/ATPase[b]	212	39	Sequence similarity
15	Component of the special vertex[b]	46	This work	Interaction with P22
16	DNA packaging[b]	46	39	PRD1 synteny, weak similarity, and protein size
17	Capsid tape measure protein (minor capsid protein)[b]	84	This work	Self-interaction and interaction with P18 (major capsid protein)
18	Major capsid protein	356	17, 39	The most abundant protein in purified Bam35c particles; homology with the X-ray structure of the PRD1 major coat protein
19	DNA packaging[b]	76	39	PRD1 synteny; the protein is present in purified Bam35c particles
20	Spike stabilizer[b]	68	This work	Interaction with P24 and P29
21	Unknown	143		
22	Component of the special vertex[b]	58	This work	Interaction with P19
23	Unknown	48		
24	Penton component[b]	91	This work	Protein size, self-interaction, interaction with the spike protein P29, and threading structural model
25	Membrane structural component	204	39	The second most abundant protein in purified Bam35c particles; transmembrane domain
26	Transglycosylase and integral membrane scaffolding protein[b]	250	25; this work	Recombinant protein characterization of identical Gil01 protein and interactions with structural proteins P24, P17, and P29
27	Unknown	170		
28	Spike[b]	304	39	Local alignment with PRD1 protein P5 and protein size
29	Spike[b]	293	17	Threading on PRD1
30	Transglycosylase	265	25	Recombinant protein characterization of identical Gil01 protein
31	Unknown	40		
32	Part of P30 transglycosylase active complex[b]	103	This work	Self-interaction and interaction with whole protein P30 (analogy with reference 54)

[a]See Table S1 in the supplemental material for more details.
[b]Suggested function.
[c]Evidence supporting the shown or proposed functions.

(10.7 kDa) is similar to that of the penton protein of PRD1 (P31, 13.7 kDa) and that protein P24 interacts with itself and with the spike protein P29, we hypothesized that protein P24 of Bam35 is the penton protein. This hypothesis was also supported by the structural model of P24 obtained using PRD1 P31 as a template (Fig. 7B).

The suggested Bam35 spike proteins, P28 and P29, as mentioned above, interacted with each other and also showed self-interactions and multiple interactions with the proposed capsid tape measure protein, P17. Moreover, P29 interacted with P24, as well as membrane proteins, like P25, P26, or P30 (Fig. 5). Protein P28 (32.4 kDa) has a size similar to that of the PRD1 ortholog (P5, 34.4 kDa), which forms a trimer in the viral spike. However, the other spike component, P29 (32.7 kDa), has a molecular mass half of that of its counterpart in PRD1 (P2, 63.8 kDa). In the viral particle of PRD1, the P2 protein is found in a monomer form (52). However, our results indicated that P29 of Bam35 can interact with itself, which would allow it to form protein complexes, and as a consequence, the morphology of its spikes should differ from that of PRD1 spikes.

Regarding the PPIs between the components of the special vertex through which the DNA is packaged into the viral particle, we observed that the DNA packaging protein P19 (8) interacts with P22, which also interacts with the membrane protein P15
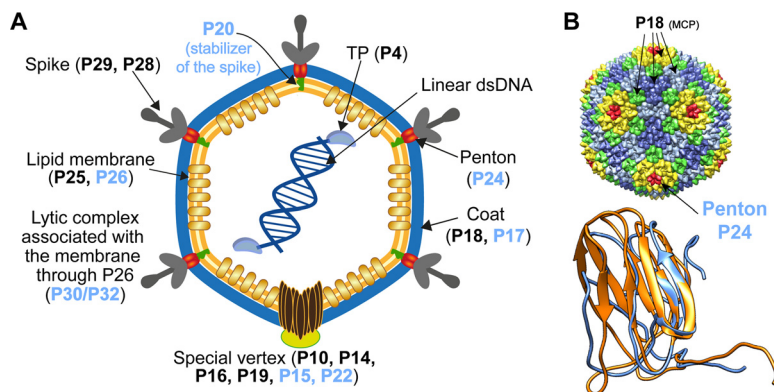
FIG 7 Model proposed for the Bam35 viral particle. (A) Schematic representation of the Bam35 viral particle in which the proposed or known localization of each of its proteins is indicated. The proteins postulated through interpretation of the data obtained in the present study are indicated in blue. (B) Capsid morphology of PRD1 obtained by X-ray crystallography (PDB accession number 1W8X) (19) and used as a model for the Bam35 capsid. The icosahedral unit contains 12 copies of the major capsid protein (P18) arranged as 4 trimers, represented in yellow, green, blue, and cyan, respectively. The Bam35 penton (red) is probably formed by protein P24, which was modeled (blue) using the PRD1 ortholog (P31; PDB accession number 1W8X; chain N; orange) as a template (C score, −1.87; TM score, 0.49 ± 0.13). The structural model was generated with the I-Tasser server (65), and structures were aligned using the MatchMaker algorithm, implemented at the University of California, San Francisco (UCSF), in the Chimera system (66). dsDNA, double-stranded DNA; MCP, major capsid protein.

(Fig. 5). These interactions would imply the localization of P22 and P15 in the special vertex. The presence of protein P22 in this vertex is in agreement with the function of DNA delivery proposed for its homolog in AP50 (51). On the other hand, protein P14, placed in the special vertex of Bam35 (8), is associated with P22 through the interaction with the transglycosylase protein P26 (26) (Fig. 5).

Membrane and lytic proteins. As we expected, the results obtained with the proteins without the transmembrane domain differed from the ones observed with the full-length proteins. This may be due to the following: (i) the localization of fusion proteins containing transmembrane domains is different from that of soluble constructs, (ii) there are differences between the tertiary structures of the full-length protein and the short version of the protein, which could expose internal domains to the surface, or (iii) the domain removed is responsible for the observed interaction, as in the case of P21 or P19, whose truncated forms did not show any interaction.

The map obtained links P20′ with proteins of unknown function: P3; P24, suggested here to be the penton protein; and P29, the spike element (Fig. 5). Therefore, the PPIs detected, together with the presence of a transmembrane domain, make P20 the only protein that could be responsible for the stabilization of the spikes, implying a role similar to that of P16 in PRD1 (20). However, these interactions were rather weak (i.e., they were suppressed at low 3AT concentrations), and therefore, additional studies would be necessary to confirm that role.

The full-length transglycosylase protein P26 also gave rise to results different from those obtained with its short version (Fig. 5). Thus, the interactions of P26 with P21 and P22 were not observed with P26′, which suggests that P26 is linked to these proteins through its amino acids 177 to 250, a region that contains the transmembrane motif (amino acids 177 to 199). The fact that P21 also contains a predicted transmembrane domain suggests an interaction in the context of the virus inner membrane, whereas P22 would interact with P26 through its 50 C-terminal amino acids. However, the possibility of nonspecific hydrophobic interactions involving P26 residues 177 to 250 cannot be ruled out.

The variant P26′ interacted strongly with itself and with the proteins P17, P24, P29, P30, and P32. In addition, its relation to the spike protein P29 is reinforced by previous evidence that indicated that the Bam35 virion is associated with external peptidoglycan hydrolases (26). In the same way, protein P30 may also be localized in the virion due to

its interactions with P26′ and P29 (see below). All these data suggest that protein P26 not only would have a lytic function but also would be implicated in more functions, either during morphogenesis of the viral particle or as a scaffold protein for other structural elements from the inner membrane and the viral capsid.

Bam35 P30 is a muramidase highly conserved among related tectiviruses and also shows homology with other endolysins from Gram-positive bacteria (25, 53). The P30-coding sequence encloses two additional annotated internal ORFs, 31 and 32, although there is no evidence of their actual translation (39). ORF31 spans nucleotides 148 to 527 in a +1 frame of the P30-coding sequence, and it did not participate in any interaction. P32 is constituted by the C-terminal domain of P30 (amino acids 163 to 265) and contains a putative peptidoglycan binding motif. P30 and P32 showed self-interaction and also interact with each other, findings which suggest that both proteins may be organized in an oligomeric lytic complex. The activity of this complex might require both proteins, as in the case for a *Clostridium* endolysin recently reported (54), which also shows partial homology with P30. On the other hand, P30, but not P32, interacts with the spike protein P29, which indicates that the P30 N-terminal region (amino acids 1 to 162) would be required for that PPI. Furthermore, according to the protein interaction network, this complex might be present in the viral particle by the interaction with P26 (Table 1 and Fig. 5).

Replication and cycle regulation proteins. Although we have previously demonstrated the functional interaction between the DNA polymerase (P5) and the terminal protein (P4) of Bam35 (29), other techniques, such as cosedimentation by glycerol gradient ultracentrifugation (unpublished data) or the method of screening used in this study, were not able to detect it. This probably indicates that the protein-primed replication initiation is achieved with a weak fleeting interaction. However, the interaction of the terminal protein with itself was detected (Fig. 5). This result could involve the interaction between the free terminal protein and the so-called parental terminal protein covalently bound to the 5′ ends of the genome during the recognition of the replication origin. A similar mechanism has been also proposed for Φ29, since some mutations in its terminal protein affect the recognition of the replication origin (55–57).

The results obtained showed a PPI between the viral TP and P1 that was confirmed by pulldown coimmunoprecipitation assays (Fig. 6). Bam35 P1 is conserved among tectiviruses from Gram-positive bacteria and contains a predicted helix-turn-helix DNA-binding motif similar to the helix-turn-helix DNA-binding motif found in the MerR superfamily of transcription regulators (58), which mediates the activation or the repression of transcription through its ability to distort the DNA helix. According to this, the P1-TP interaction may be important to attract P1 to the origin of replication, where P1 might play an additional role, such as facilitating the initiation of replication and/or later steps.

Regarding the regulatory proteins of the Bam35 life cycle, we found that P6, previously suggested to be a possible lytic cycle repressor (58), interacts with different proteins, especially P29, P24, and P30 (Fig. 5). However, additional studies are necessary to find a biological explanation for these interactions. On the other hand, P7, which regulates the lysogenic cycle through the interaction with the host LexA repressor (59), shows a strong capacity to interact with itself (Fig. 5). This suggests that P7 multimerization may be involved in the regulation of the bacteriophage cycle by modulating its capacity to bind to DNA or LexA; i.e., the complex of P7 could have a higher or a lower affinity for the LexA repressor than for its monomer. Hence, the P7 complex could decrease or increase the binding of LexA to DNA. Finally, similarly to P6, P7 interacts with P24 and P26′, which would suggest its presence in the viral particle and, thus, its involvement in very early infection events. Further studies are necessary to explain the biological role of them.

Conclusion and perspectives. The genomewide protein interactome of Bam35 provides a comprehensive basis that paves the way for further work on specific proteins or biological processes. The Y2H screening performed here provides a general first

insight into the interactions of the proteins encoded by the genome of Bam35. This approach opens new questions, such as the possible localization of P6 and P7 within the virion. Moreover, some interactions involved proteins whose functions remain obscure, such as P3, P8, or P9, but they do suggest some directions for future work.

The analysis of the protein interaction network obtained allowed us to suggest the functions of three ORFan proteins of unknown function and the localization in the virion of five other proteins (Table 2 and Fig. 7). Given the similarities among the bacteriophages of the *Tectiviridae* family, our data provide starting points for the analysis of other members of this family.

MATERIALS AND METHODS

Cloning the bacteriophage Bam35 ORFs into Gateway entry vector pDONR/Zeo. The DNA sequence of phage Bam35 was obtained from the NCBI genome database (accession number NC_005258.1), and the primers used to amplify predicted ORFs were designed using Geneious software (60). The primers had lengths of 20 to 30 nucleotides complementary to the ORF of interest, and the endogenous stop codons were removed (see Table S2 in the supplemental material). The *attB1* sequence (5′-AAAAAGCAGGCTTA-3′) and the *attB2* segment (5′-AGAAAGCTGGGTG-3′) were added at the 5′ end of each forward or reverse primer, respectively.

The transmembrane domains of the proteins encoded by the Bam35 genome were predicted using TMHMM software (48). Short versions of the ORFs without their transmembrane domain were generated using the oligonucleotides marked in red in Table S2.

All full-length Bam35 ORFs and their short versions were amplified by PCR using the primers in Table S2 and the Bam35 genome as a template. Amplifications were performed with Kapa Hi-Fi DNA polymerase (Kapa Biosystems) following the manufacturer's recommendations. The PCR products were checked in a 0.7% agarose gel and used as a template for a second round of PCR with primers attB1 and attB2 (Table S2), generating the full-length *attB1* and *attB2* sites flanking the ORFs.

The products of the second PCR were recombined into the entry vector pDONR/Zeo (Invitrogen) by using the BP Clonase II enzyme mix (Invitrogen). The vectors obtained were transformed into *Escherichia coli* DH5α and plated onto solid LB medium containing 50 μg/ml zeocin. To select the colonies transformed with the correct clones, we tested for the presence of the insert by colony PCR using the same primers used in the first round of PCR. The positive colonies were picked for plasmid isolation, and their inserts were sequenced using the forward primer M13 (Table S2).

Subcloning into yeast two-hybrid expression vectors. All the Bam35 ORFs cloned in pDONR/Zeo were subcloned into yeast two-hybrid expression vectors by using the LR Clonase II enzyme mix (Invitrogen). The bait vectors used were pGBGT7g (gentamicin resistant [Gen^r]) and pGBKCg (kanamycin resistant [Kan^r]), and the prey vectors used were pGADT7g (ampicillin resistant [Amp^r]) and pGADCg (Amp^r) (44). Thus, a collection of 4 vectors was generated with each cloned ORF. The vectors obtained were transformed into *E. coli* DH5α and plated onto solid LB medium with the necessary antibiotic. One colony of each transformation was selected for plasmid isolation, and the presence of the insert was retested by PCR with the T7 forward primer and the attB2* reverse primer (Table S2) for cloning in pGADT7g and pGBGT7g and with the attB1* forward primer and attB2* reverse primer for cloning in pGADCg and pGBKCg (Table S2). Additionally, some of the clones were chosen at random to be resequenced with the T7 forward primer for the inserts in pGBGT7g and pGADT7g or with the attB1* forward primer for the inserts in pGADCg and pGBKCg. We obtained all the clones except pGBKCg::ORF16 (Table S3).

Yeast two-hybrid screening. *Saccharomyces cerevisiae* AH109 and Y187 were transformed with bait and prey vectors, respectively, following the protocol of Mehla et al. (61). Yeast cells containing the bait vector were selected on solid medium without tryptophan, while solid medium lacking leucine was used for selection of the prey vector. Thus, we obtained all the yeast clones except pGBKCg::ORF16, pGADCg::ORF9, and pGADC::ORF26 (Table S4). Once the transformed yeast cells were selected, we performed mating between cells containing the bait vectors and cells containing the prey vectors to obtain diploid yeast cells with the following vector pairs: pGBKCg/pGADCg, pGBKCg/pGADT7g, pGBGT7g/pGADCg, and pGBGT7g/pGADCg. The diploid cells were selected in solid medium without tryptophan and leucine.

Finally, *HIS3* was used as a reporter gene to detect protein-protein interactions. As this gene encodes an imidazole glycerol phosphate dehydratase necessary for histidine biosynthesis and the yeast strains used in that study are auxotrophic for this amino acid, the interactions were detected through analysis of yeast growth in a selective solid medium without tryptophan, leucine, and histidine. Additionally, we used a competitive inhibitor of the *HIS3* product called 3-amino-1,2,4-triazole (3AT), which suppresses low levels of His3 activity (resulting from low levels of transcription). This increases the stringency of selection and thus reduces false-positive interactions (50). Thus, 3AT was added to the medium at a concentration the same as or higher than that previously established through the study of bait autoactivation (Table S5). The protein interaction network of Bam35 was represented using Cytoscape software (62), and subsequent modifications for clarity purposes were made with the Adobe Illustrator program.

Expression of fusion proteins HA-P1 and P1-HA and analysis of direct interaction with the viral TP by pulldown coimmunoprecipitation. ORF1 of Bam35 was amplified by PCR using the P1_T7 forward and reverse primers (Table S2), Bam35 genomic DNA as a template, and Vent DNA polymerase (New England BioLabs). The PCR product was cloned into the NdeI and BamHI sites of the pT7-7 plasmid

(63), producing the pT7-7::B35P1 vector. This plasmid was used to construct the vector pT7-7::B35P1HA, which expresses the protein P1 linked to the HA tag by its C-terminal end (P1-HA) by insertion of an HA-coding adaptor duplex (P1_HA_T7; Table S2) in the BamHI and HindIII sites. To generate plasmid pT7-7::B35HAP1, which expresses protein P1 of Bam35 linked to the HA tag by its N-terminal end (HA-P1), we again amplified ORF1 using HA_P1_T7 primers, which contain an in-frame HA motif, and the PCR product was cloned into the NdeI and BamHI sites of the pT7-7 vector. In all cases, the constructions cloned were sequenced.

To induce the expression of the HA-P1 and P1-HA proteins, cultures of *E. coli* BL21(DE3) harboring the corresponding expression vector or the pT7-7 empty plasmid were grown in ZYM-5052 autoinduction medium (64) with 150 μg/ml of ampicillin at 30°C for 16 h. After induction, cells were collected, resuspended in 500 μl sterile phosphate-buffered saline (PBS), pH 8, supplemented with complete protease inhibitor (cOmplete Ultra; Sigma), and incubated with 1 mg/ml of lysozyme (Sigma) for 20 min on ice. We used PBS at pH 8 because of the high isoelectric point of Bam35 TP, which may affect its function *in vitro* (29). Then, the cells were disrupted by sonication and the lysate was subsequently treated with 375 units of nuclease (Benzonase; Sigma) in the presence of 2.5 mM $MgCl_2$ for 30 min at room temperature to rule out the possibility of a DNA-mediated indirect interaction. Finally, cellular debris was removed by centrifugation.

P1 immunoprecipitation was performed using Pierce anti-HA agarose (Thermo Scientific) according to the manufacturer's recommendations. Briefly, cell-free lysates of cultures carrying the empty pT7-7, pT7-7::B35HAP1, or pT7-7::B35P1HA vector, obtained as indicated above, were incubated with 50 μl of anti-HA agarose at 4°C for 18 h on a rotating wheel. After low-speed centrifugation, the unbound proteins were removed by centrifugation and the agarose beads were washed three times with 10 volumes of PBS, pH 8, with 0.05% Tween 20 (PBS-T; Sigma) for 5 min at 4°C. Afterwards, a mixture of 2 μg of purified Bam35 terminal protein (29) and 30 μg of bovine serum albumin (BSA; Sigma) in 500 μl of PBS-T was added, and the mixture was incubated at 4°C for 2 h on a rotating wheel. After collection of the supernatant containing unbound proteins, the agarose was washed as described above. Finally, the bound proteins were eluted by incubation with 50 μl of 1× Laemmli SDS-PAGE sample buffer (4% β-mercaptoethanol, 1.8% [wt/vol] SDS, 12% glycerol, 120 mM Tris HCl, pH 6.8, 0.005% bromophenol blue) for 5 min at 95°C.

Samples were analyzed by SDS-PAGE followed by Coomassie blue staining and Western blotting with specific antibodies against TP using standard methods. Briefly, gels were transferred onto a polyvinylidene difluoride (PVDF) membrane (Sigma) and detected using an anti-TP serum raised in rabbits (dilution, 1:5,000) and a goat anti-rabbit immunoglobulin-horseradish peroxidase conjugate antibody (GE Healthcare). The proteins were then detected with an enhanced chemiluminescence system (GE Healthcare) according to the manufacturer's recommendations.

SUPPLEMENTAL MATERIAL

Supplemental material for this article may be found at https://doi.org/10.1128/JVI .00870-17.

SUPPLEMENTAL FILE 1, XLSX file, 0.1 MB.

REFERENCES

1. Olsen RH, Siak JS, Gray RH. 1974. Characteristics of PRD1, a plasmid-dependent broad host range DNA bacteriophage. J Virol 14:689–699.
2. Gillis A, Mahillon J. 2014. Prevalence, genetic diversity, and host range of tectiviruses among members of the Bacillus cereus group. Appl Environ Microbiol 80:4138–4152. https://doi.org/10.1128/AEM.00912-14.
3. Verheust C, Fornelos N, Mahillon J. 2005. GIL16, a new gram-positive tectiviral phage related to the *Bacillus thuringiensis* GIL01 and the *Bacillus cereus* pBClin15 elements. J Bacteriol 187:1966–1973. https://doi.org/10.1128/JB.187.6.1966-1973.2005.
4. Nagy E. 1974. A highly specific phage attacking *Bacillus anthracis* strain Sterne. Acta Microbiol Acad Sci Hung 21:257–263.
5. Schuch R, Pelzek AJ, Kan S, Fischetti VA. 2010. Prevalence of *Bacillus anthracis*-like organisms and bacteriophages in the intestinal tract of the earthworm *Eisenia fetida*. Appl Environ Microbiol 76:2286–2294. https://doi.org/10.1128/AEM.02518-09.
6. Gillis A, Mahillon J. 2014. Phages preying on *Bacillus anthracis*, *Bacillus cereus*, and *Bacillus thuringiensis*: past, present and future. Viruses 6:2623–2672. https://doi.org/10.3390/v6072623.
7. Jalasvuori M, Palmu S, Gillis A, Kokko H, Mahillon J, Bamford JK, Fornelos N. 2013. Identification of five novel tectiviruses in *Bacillus* strains: analysis of a highly variable region generating genetic diversity. Res Microbiol 164:118–126. https://doi.org/10.1016/j.resmic.2012.10.011.

8. Stromsten NJ, Benson SD, Burnett RM, Bamford DH, Bamford JK. 2003. The *Bacillus thuringiensis* linear double-stranded DNA phage Bam35, which is highly similar to the *Bacillus cereus* linear plasmid pBClin15, has a prophage state. J Bacteriol 185:6985–6989. https://doi.org/10.1128/JB.185.23.6985-6989.2003.

9. Gaidelyte A, Jaatinen ST, Daugelavicius R, Bamford JK, Bamford DH. 2005. The linear double-stranded DNA of phage Bam35 enters lysogenic host cells, but the late phage functions are suppressed. J Bacteriol 187:3521–3527. https://doi.org/10.1128/JB.187.10.3521-3527.2005.

10. Fischetti VA. 2011. Exploiting what phage have evolved to control gram-positive pathogens. Bacteriophage 1:188–194. https://doi.org/10.4161/bact.1.4.17747.

11. Kan S, Fornelos N, Schuch R, Fischetti VA. 2013. Identification of a ligand on the Wip1 bacteriophage highly specific for a receptor on *Bacillus anthracis*. J Bacteriol 195:4355–4364. https://doi.org/10.1128/JB.00655-13.

12. Krupovic M, Koonin EV. 2015. Polintons: a hotbed of eukaryotic virus, transposon and plasmid evolution. Nat Rev Microbiol 13:105–115. https://doi.org/10.1038/nrmicro3389.

13. Koonin EV, Krupovic M, Yutin N. 2015. Evolution of double-stranded DNA viruses of eukaryotes: from bacteriophages to transposons to giant viruses. Ann N Y Acad Sci 1341:10–24. https://doi.org/10.1111/nyas.12728.

14. Oksanen HM, Bamford DH. 2012. Family *Tectiviridae*, p 317–321. *In* King AMQ, Adams MJ, Carstens EB, Lefkowitz EJ (ed), Virus taxonomy. Classification and nomenclature of viruses. Ninth report of the International Committee on Taxonomy of Viruses. Elsevier Academic Press, San Diego, CA.

15. Butcher SJ, Bamford DH, Fuller SD. 1995. DNA packaging orders the membrane of bacteriophage PRD1. EMBO J 14:6078–6086.

16. Cockburn JJ, Abrescia NG, Grimes JM, Sutton GC, Diprose JM, Benevides JM, Thomas GJ, Jr, Bamford JK, Bamford DH, Stuart DI. 2004. Membrane structure and interactions with protein and DNA in bacteriophage PRD1. Nature 432:122–125. https://doi.org/10.1038/nature03053.

17. Laurinmaki PA, Huiskonen JT, Bamford DH, Butcher SJ. 2005. Membrane proteins modulate the bilayer curvature in the bacterial virus Bam35. Structure 13:1819–1828. https://doi.org/10.1016/j.str.2005.08.020.

18. Laurinavicius S, Bamford DH, Somerharju P. 2007. Transbilayer distribution of phospholipids in bacteriophage membranes. Biochim Biophys Acta 1768:2568–2577. https://doi.org/10.1016/j.bbamem.2007.06.009.

19. Abrescia NG, Cockburn JJ, Grimes JM, Sutton GC, Diprose JM, Butcher SJ, Fuller SD, San Martin C, Burnett RM, Stuart DI, Bamford DH, Bamford JK. 2004. Insights into assembly from structural analysis of bacteriophage PRD1. Nature 432:68–74. https://doi.org/10.1038/nature03056.

20. Jaatinen ST, Viitanen SJ, Bamford DH, Bamford JK. 2004. Integral membrane protein P16 of bacteriophage PRD1 stabilizes the adsorption vertex structure. J Virol 78:9790–9797. https://doi.org/10.1128/JVI.78.18.9790-9797.2004.

21. Stromsten NJ, Bamford DH, Bamford JK. 2003. The unique vertex of bacterial virus PRD1 is connected to the viral internal membrane. J Virol 77:6314–6321. https://doi.org/10.1128/JVI.77.11.6314-6321.2003.

22. Mindich L, Bamford D, Goldthwaite C, Laverty M, Mackenzie G. 1982. Isolation of nonsense mutants of lipid-containing bacteriophage PRD1. J Virol 44:1013–1020.

23. Pakula TM, Savilahti H, Bamford DH. 1989. Comparison of the amino acid sequence of the lytic enzyme from broad-host-range bacteriophage PRD1 with sequences of other cell-wall-peptidoglycan lytic enzymes. Eur J Biochem 180:149–152. https://doi.org/10.1111/j.1432-1033.1989.tb14625.x.

24. Caldentey J, Hanninen AL, Bamford DH. 1994. Gene XV of bacteriophage PRD1 encodes a lytic enzyme with muramidase activity. Eur J Biochem 225:341–346. https://doi.org/10.1111/j.1432-1033.1994.00341.x.

25. Verheust C, Fornelos N, Mahillon J. 2004. The *Bacillus thuringiensis* phage GIL01 encodes two enzymes with peptidoglycan hydrolase activity. FEMS Microbiol Lett 237:289–295.

26. Gaidelyte A, Cvirkaite-Krupovic V, Daugelavicius R, Bamford JK, Bamford DH. 2006. The entry mechanism of membrane-containing phage Bam35 infecting *Bacillus thuringiensis*. J Bacteriol 188:5925–5934. https://doi.org/10.1128/JB.00107-06.

27. Caldentey J, Blanco L, Savilahti H, Bamford DH, Salas M. 1992. *In vitro* replication of bacteriophage PRD1 DNA. Metal activation of protein-primed initiation and DNA elongation. Nucleic Acids Res 20:3971–3976.

28. Caldentey J, Blanco L, Bamford DH, Salas M. 1993. *In vitro* replication of bacteriophage PRD1 DNA. Characterization of the protein-primed initiation site. Nucleic Acids Res 21:3725–3730.

29. Berjón-Otero M, Villar L, Salas M, Redrejo-Rodríguez M. 2016. Disclosing

30. Salas M. 1991. Protein-priming of DNA replication. Annu Rev Biochem 60:39–71. https://doi.org/10.1146/annurev.bi.60.070191.000351.

31. Salas M, Holguera I, Redrejo-Rodriguez M, de Vega M. 2016. DNA-binding proteins essential for protein-primed bacteriophage Φ29 DNA replication. Front Mol Biosci 3:37. https://doi.org/10.3389/fmolb.2016.00037.

32. Hoeben RC, Uil TG. 2013. Adenovirus DNA replication. Cold Spring Harb Perspect Biol 5:a013003. https://doi.org/10.1101/cshperspect.a013003.

33. Klassen R, Meinhardt F. 2007. Linear protein-primed replicating plasmids in eukaryotic microbes, p 187–226. *In* Microbial linear plasmids. Springer, Berlin, Germany. https://doi.org/10.1007/7171_2007_095.

34. Savilahti H, Caldentey J, Lundstrom K, Syvaoja JE, Bamford DH. 1991. Overexpression, purification, and characterization of *Escherichia coli* bacteriophage PRD1 DNA polymerase. In vitro synthesis of full-length PRD1 DNA with purified proteins. J Biol Chem 266:18737–18744.

35. Berjón-Otero M, Villar L, de Vega M, Salas M, Redrejo-Rodríguez M. 2015. DNA polymerase from temperate phage Bam35 is endowed with processive polymerization and abasic sites translesion synthesis capacity. Proc Natl Acad Sci U S A 112:E3476–E3484. https://doi.org/10.1073/pnas.1510280112.

36. Zhu W, Ito J. 1994. Purification and characterization of PRD1 DNA polymerase. Biochim Biophys Acta 1219:267–276. https://doi.org/10.1016/0167-4781(94)90048-5.

37. Pakula TM, Caldentey J, Serrano M, Gutiérrez C, Hermoso JM, Salas M, Bamford DH. 1990. Characterization of a DNA binding protein of bacteriophage PRD1 involved in DNA replication. Nucleic Acids Res 18:6553–6557. https://doi.org/10.1093/nar/18.22.6553.

38. Pakula TM, Caldentey J, Gutiérrez C, Olkkonen VM, Salas M, Bamford DH. 1993. Overproduction, purification, and characterization of DNA-binding protein P19 of bacteriophage PRD1. Gene 126:99–104. https://doi.org/10.1016/0378-1119(93)90595-T.

39. Ravantti JJ, Gaidelyte A, Bamford DH, Bamford JK. 2003. Comparative analysis of bacterial viruses Bam35, infecting a gram-positive host, and PRD1, infecting gram-negative hosts, demonstrates a viral lineage. Virology 313:401–414. https://doi.org/10.1016/S0042-6822(03)00295-2.

40. Saren AM, Ravantti JJ, Benson SD, Burnett RM, Paulin L, Bamford DH, Bamford JK. 2005. A snapshot of viral evolution from genome analysis of the Tectiviridae family. J Mol Biol 350:427–440. https://doi.org/10.1016/j.jmb.2005.04.059.

41. Grazziotin AL, Koonin EV, Kristensen DM. 2017. Prokaryotic virus orthologous groups (pVOGs): a resource for comparative genomics and protein family annotation. Nucleic Acids Res 45:D491–D498. https://doi.org/10.1093/nar/gkw975.

42. Delattre H, Souiai O, Fagoonee K, Guerois R, Petit MA. 2016. Phagonaute: a web-based interface for phage synteny browsing and protein function prediction. Virology 496:42–50. https://doi.org/10.1016/j.virol.2016.05.007.

43. Mehla J, Caufield JH, Uetz P. 2015. The yeast two-hybrid system: a tool for mapping protein-protein interactions. Cold Spring Harb Protoc 2015:425–430. https://doi.org/10.1101/pdb.top083345.

44. Stellberger T, Hauser R, Baiker A, Pothineni VR, Haas J, Uetz P. 2010. Improving the yeast two-hybrid system with permutated fusions proteins: the varicella zoster virus interactome. Proteome Sci 8:8. https://doi.org/10.1186/1477-5956-8-8.

45. Rajagopala SV, Casjens S, Uetz P. 2011. The protein interaction map of bacteriophage lambda. BMC Microbiol 11:213. https://doi.org/10.1186/1471-2180-11-213.

46. Mehla J, Dedrick RM, Caufield JH, Siefring R, Mair M, Johnson A, Hatfull GF, Uetz P. 2015. The protein interactome of mycobacteriophage Giles predicts functions for unknown proteins. J Bacteriol 197:2508–2516. https://doi.org/10.1128/JB.00164-15.

47. Hauser R, Sabri M, Moineau S, Uetz P. 2011. The proteome and interactome of *Streptococcus pneumoniae* phage Cp-1. J Bacteriol 193:3135–3138. https://doi.org/10.1128/JB.01481-10.

48. Krogh A, Larsson B, von Heijne G, Sonnhammer EL. 2001. Predicting transmembrane protein topology with a hidden Markov model: application to complete genomes. J Mol Biol 305:567–580. https://doi.org/10.1006/jmbi.2000.4315.

49. Bolotin A, Gillis A, Sanchis V, Nielsen-LeRoux C, Mahillon J, Lereclus D, Sorokin A. 2017. Comparative genomics of extrachromosomal elements in *Bacillus thuringiensis* subsp. *israelensis*. Res Microbiol 168:331–344. https://doi.org/10.1016/j.resmic.2016.10.008.

50. Bruckner A, Polge C, Lentze N, Auerbach D, Schlattner U. 2009. Yeast

early steps of protein-primed genome replication of the Gram-positive tectivirus Bam35. Nucleic Acids Res 44:9733–9744.

two-hybrid, a powerful tool for systems biology. Int J Mol Sci 10: 2763–2788. https://doi.org/10.3390/ijms10062763.

51. Sozhamannan S, McKinstry M, Lentz SM, Jalasvuori M, McAfee F, Smith A, Dabbs J, Ackermann HW, Bamford JK, Mateczun A, Read TD. 2008. Molecular characterization of a variant of *Bacillus anthracis*-specific phage AP50 with improved bacteriolytic activity. Appl Environ Microbiol 74:6792–6796. https://doi.org/10.1128/AEM.01124-08.

52. Xu L, Butcher SJ, Benson SD, Bamford DH, Burnett RM. 2000. Crystallization and preliminary X-ray analysis of receptor-binding protein P2 of bacteriophage PRD1. J Struct Biol 131:159–163. https://doi.org/10.1006/jsbi.2000.4275.

53. Loessner MJ, Maier SK, Daubek-Puza H, Wendlinger G, Scherer S. 1997. Three *Bacillus cereus* bacteriophage endolysins are unrelated but reveal high homology to cell wall hydrolases from different bacilli. J Bacteriol 179:2845–2851. https://doi.org/10.1128/jb.179.9.2845-2851.1997.

54. Dunne M, Leicht S, Krichel B, Mertens HD, Thompson A, Krijgsveld J, Svergun DI, Gomez-Torres N, Garde S, Uetrecht C, Narbad A, Mayer MJ, Meijers R. 2016. Crystal structure of the CTP1L endolysin reveals how its activity is regulated by a secondary translation product. J Biol Chem 291:4882–4893. https://doi.org/10.1074/jbc.M115.671172.

55. Illana B, Zaballos A, Blanco L, Salas M. 1998. The RGD sequence in phage Φ29 terminal protein is required for interaction with Φ29 DNA polymerase. Virology 248:12–19. https://doi.org/10.1006/viro.1998.9276.

56. Serna-Rico A, Illana B, Salas M, Meijer WJ. 2000. The putative coiled coil domain of the Φ29 terminal protein is a major determinant involved in recognition of the origin of replication. J Biol Chem 275:40529–40538. https://doi.org/10.1074/jbc.M007855200.

57. Del Prado A, Villar L, de Vega M, Salas M. 2012. Involvement of residues of the Φ29 terminal protein intermediate and priming domains in the formation of a stable and functional heterodimer with the replicative DNA polymerase. Nucleic Acids Res 40:3886–3897. https://doi.org/10.1093/nar/gkr1283.

58. Fornelos N, Bamford JK, Mahillon J. 2011. Phage-borne factors and host LexA regulate the lytic switch in phage GIL01. J Bacteriol 193: 6008–6019. https://doi.org/10.1128/JB.05618-11.

59. Fornelos N, Butala M, Hodnik V, Anderluh G, Bamford JK, Salas M. 2015. Bacteriophage GIL01 gp7 interacts with host LexA repressor to enhance DNA binding and inhibit RecA-mediated auto-cleavage. Nucleic Acids Res 43:7315–7329. https://doi.org/10.1093/nar/gkv634.

60. Kearse M, Moir R, Wilson A, Stones-Havas S, Cheung M, Sturrock S, Buxton S, Cooper A, Markowitz S, Duran C, Thierer T, Ashton B, Meintjes P, Drummond A. 2012. Geneious Basic: an integrated and extendable desktop software platform for the organization and analysis of sequence data. Bioinformatics 28:1647–1649. https://doi.org/10.1093/bioinformatics/bts199.

61. Mehla J, Caufield JH, Uetz P. 2015. Mapping protein-protein interactions using yeast two-hybrid assays. Cold Spring Harb Protoc 2015:442–452. https://doi.org/10.1101/pdb.prot086157.

62. Shannon P, Markiel A, Ozier O, Baliga NS, Wang JT, Ramage D, Amin N, Schwikowski B, Ideker T. 2003. Cytoscape: a software environment for integrated models of biomolecular interaction networks. Genome Res 13:2498–2504. https://doi.org/10.1101/gr.1239303.

63. Tabor S, Richardson CC. 1985. A bacteriophage T7 RNA polymerase/promoter system for controlled exclusive expression of specific genes. Proc Natl Acad Sci U S A 82:1074–1078. https://doi.org/10.1073/pnas.82.4.1074.

64. Studier FW. 2005. Protein production by auto-induction in high density shaking cultures. Protein Expr Purif 41:207–234. https://doi.org/10.1016/j.pep.2005.01.016.

65. Roy A, Kucukural A, Zhang Y. 2010. I-TASSER: a unified platform for automated protein structure and function prediction. Nat Protoc 5:725–738. https://doi.org/10.1038/nprot.2010.5.

66. Pettersen EF, Goddard TD, Huang CC, Couch GS, Greenblatt DM, Meng EC, Ferrin TE. 2004. UCSF Chimera—a visualization system for exploratory research and analysis. J Comput Chem 25:1605–1612. https://doi.org/10.1002/jcc.20084.

67. Stabell FB, Egge-Jacobsen W, Risoen PA, Kolsto AB, Okstad OA. 2009. ORF 2 from the *Bacillus cereus* linear plasmid pBClin15 encodes a DNA binding protein. Lett Appl Microbiol 48:51–57. https://doi.org/10.1111/j.1472-765X.2008.02483.x.